

# ORTHOPROJECTION TESTS OF HYPERSPECTRAL DATA IN STEEP SLOPE ZONES

Piero Boccardo\*, Enrico Borgogno Mondino\*, Mario A. Gomasca\*\*, Luigi Perotti\*\*\*

\* DIGET, Politecnico di Torino, C.so Duca degli Abruzzi 24, 10129 Torino (ITALY)

e-mail : [enrico.borgogno@polito.it](mailto:enrico.borgogno@polito.it), [piero.boccardo@polito.it](mailto:piero.boccardo@polito.it)

\*\* CNR-IREA, Sezione di Milano, Via Bassini 15, 20133 Milano (ITALY)

e-mail: [gomasca.m@irea.cnr.it](mailto:gomasca.m@irea.cnr.it)

\*\*\*Dipartimento di Scienze della Terra, Università di Torino, Via Valperga Caluso 35, 10125 Torino (ITALY) e-mail:

[luigi.perotti@unito.it](mailto:luigi.perotti@unito.it)

**KEY WORDS:** Remote Sensing, Image Geometry, Orthoprojection, whiskbroom, accuracy, Hyper spectral, Neural network, RFM

## ABSTRACT :

Nowadays hyperspectral data are really important in the environmental field. While the advantages, due to their radiometric features are broadly documented a rigorous metric verification is still absent especially in uneven areas (mountains) where the presence of steep slopes produces strong deformations on the images that have therefore to be preventively corrected. The classification potentialities and the high number of bands of the hyperspectral data is already known by operators. Nevertheless these risk to rest unusable if a good correction of the scenes geometry is not guaranteed. The mountain zones represent a critical benchmark for both warping and orthoprojection algorithms; therefore they have been chosen during this study. Positioning accuracy (planimetric) tests have been conducted on airborne sensor MIVIS images (*Multispectral Infrared Visible Imaging Spectrometer*). Such system is based on the whiskbroom digital acquisition technology. The rigorous definition of the projective model still remains an open problem subordinated to the external orientation auxiliary data. However the sensor model problem cannot be neglected because of the strong geometric deformations of the images that can make them useless or improper for the mapping scales suggested by their average geometric resolution. This study shows some orthoprojection results obtained both by commercial software and by autonomous procedures (developed by the authors) based on self-calibrating *Rational Function Model* and on *Multi Layer Perceptron* neural network. A comparison among the different methodologies has been conducted taking care of the geometric accuracy in order to define the most appropriate map scale they could be addressed to. A MIVIS image has been select for the test, recorded with an across-valley flight on the middle Valley of Susa (Turin-Italy), where the elevation range is about 1800 meters.

## 1. INTRODUCTION

### 1.1 Main purposes

This work presents some results about geometric correction of MIVIS sensor images acquired over a mountain region where image distortions are really heavy and they cannot be neglected. Two non-parametric correction methods have been selected: RFM (Rational Function Model) and a prototypal one based on a NN (Neural Network) approach. Both of them relate image and terrain coordinates considering also the terrain elevation data for relief displacement minimization.

Tests demonstrate that many factors determine the quality of the final result as the number and the distribution of the GCP (Ground Control Points), DEM quality, algorithm implementation, presence of unknown distortions. Non-parametric methods, alternative to the rigorous ones, allow to proceed to correct all the distortion globally without knowledge of any auxiliary flight information.

Different geometric correction tests have been performed in order to define how the two methods perform varying internal parameters. This is intended to state their reliability for an operative approach.

### 1.2 MIVIS hyper-spectral sensor

LARA-CNR (Aerial Laboratory for Environmental Researches of Italian National Research Council) has developed and assembled the MIVIS hyper-spectral sensor; it operates with

high geometric and spectral resolution (depending on the flying height and generally ranging from 5 to 2m). The MIVIS whiskbroom sensor can record 102 bands. All the bands belongs to the spectral range from the visible to the thermal infrared, including the near and medium infra-red.

MIVIS is a modular instrument consisting in four spectrometers which simultaneously measure the radiance from the Earth's surface for a total of 102 spectral bands: 20 in the visible spectral region (0.43-0.83 $\mu$ m), 8 in the near infrared (1.15-1.55 $\mu$ m), 64 in the middle infrared (2.0-2.5 $\mu$ m) and 10 in the thermal infrared (8.2-12.7 $\mu$ m). The chosen spectral ranges can satisfy operational requirements for botany, agrarian sciences, geology, pedology and all the sciences dealing with the territory surveying. As far as geology/geomorphology is concerned, if rigorous geometric correction and spectral calibration have done, MIVIS sensor can be effectively be used for analyzing evident superficial features (qualitative and quantitative approach ) that could be involved in some type of unstable phenomena.

Spectrometer	Bands	Channels	Lower Limit (nm)	Upper Limit (nm)	Band (nm)
1	1-20	20	430	830	20
2	21-28	8	1150	1550	50
3	29-92	64	1983	2478	9
4	93-102	10	8180	12700	340÷540

Table 1 - MIVIS images features.

### 1.2 Available images and software elaboration

The geometric correction operations were performed on two MIVIS images from an area of the Susa Valley, Piemonte Region in Italy. They were taken by flights, transversal to the valley, as shown in figure 1.

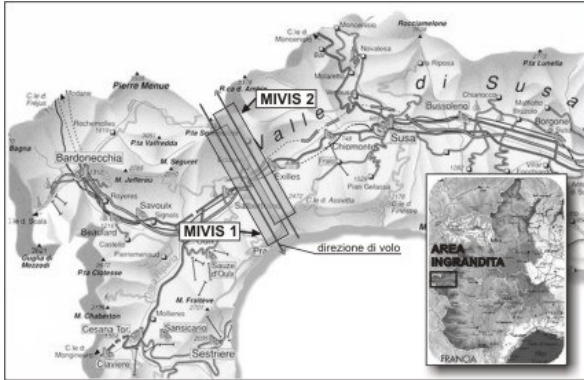


Figure 1 -Test area for the MIVIS images acquired.

The test area is characterized by a notable elevation variability: from quota 1000 m a.s.l. along the valley to a maximum quota above 3000 m a.s.l., sometimes with steep areas (see figure 2). Such situation can widely represent a generic example of a mountainous area.

Official orthoimages and the Piemonte Regional Map (scale 1:10000) of the area have been used as cartographic references for the collimation of the GCPs and of the Check Points (CPs) and for operating a qualitative analysis of the geometric correction results.

At last, the DEM of the study area has been used, grid 50m x

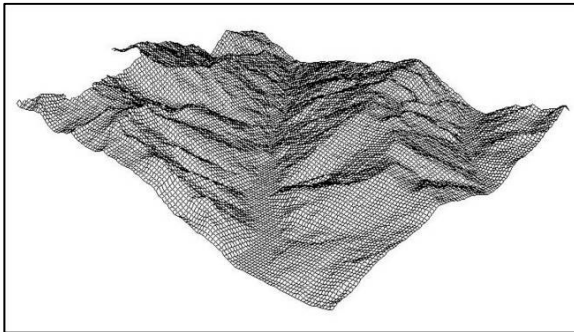


Figure 2 – 3D view of the Digital Elevation Model of MIVIS test zone: the figure shows the strong orographic variability.

50m, for the extraction of the elevation information of the GCPs and CPs and as auxiliary data required by the RFM and NN correction methods.

RFM approach has been carried out by the commercial software OrthoEngine PCI Geomatica 8.2 software. The experimental method based on NN has been instead implemented in IDL (*Interactive Data Language*) language as far as data preparation and orthoimage generation is concerned, and in MATLAB language for neural network training and network adoption for the estimation of image coordinates from terrain coordinates as successively shown.

	M I V I S 1	M I V I S 2
Acquisition data	26/07/1999	26/07/1999
Acquisition time	11:45	11:52
Flight Height	17100 ft (5212 m a.s.l.)	17500 ft (5334 m a.s.l.)
Rows number	4000	4001
Columns number	755	755
Spectral Resolution	102 bands	102 bands
Geometric Resolution	4 – 8 m	4 – 8 m
Preprocessing level	0	0

Table 2 – Test MIVIS images features.

### 1.3 Orthoprojection problems

When dealing with territorial applications it is always important to correctly approach the scale mapping problem. This means that ground objects positioning must be coherent for all the used data (often coming from different sources and reference map systems). Such problem can be easily solved with geocoded data such as ancillary and cartographic ones. Not so easy is to face the problem of MIVIS data geocoding reaching an acceptable planimetric positioning tolerance (depending on the nominal scale of the base map that will be adopted and on the final application required). Therefore MIVIS image geocoding is a delicate step to go through; complexities are due both to the whiskbroom MIVIS sensor model, which introduces many deformations to take care of, and to the moved surface of the area. Scene geometry has therefore to be corrected. Usual procedure based on simple flat transformations cannot model such geometry especially in a mountain region as the study area is. Orthoprojection has to be considered in order to make MIVIS data suitable for the data integration and analysis.

Since MIVIS raw data often are released to the final user without any metadata about attitude ad position time-dependent of the sensor, a non parametric approach has to be applied. Our first task has been to investigate which solution was the most appropriate. We considered successively two orthoprojection methods.

## 2. GEOMETRIC CORRECTION METHODS

### 2.1 Rational Function Model

This is the most famous and used non-parametric model. It is present within almost every remote sensing commercial software. It allows to relate image coordinates ( $\xi, \eta$ ) with object-terrain 3D coordinate (X,Y,Z) through rational polynomials as shown in (1):

$$\xi = \frac{P_a(X, Y, Z)}{P_b(X, Y, Z)} \quad (1)$$

$$\eta = \frac{P_c(X, Y, Z)}{P_d(X, Y, Z)}$$

$P_a, P_b, P_c, P_d$ , are polynomials of maximum 3° degree (78 parameters to be estimated) whose equations are (2) o (3):

$$P_a(X, Y, Z) = a_0 + a_1X + a_2Y + a_3Z + a_4X^2 + a_5XY + \dots + a_{17}Y^2Z + a_{18}YZ^2 + a_{19}Z^3 \quad (2)$$

$$P_a(X, Y, Z) = \sum_{i=0}^{m_1} \sum_{j=0}^{m_2} \sum_{k=0}^{m_3} a_{ijk} X^i Y^j Z^k \quad (3)$$

$$0 \leq m_1 \leq 3; 0 \leq m_2 \leq 3; 0 \leq m_3 \leq 3 \text{ e } m_1 + m_2 + m_3 \leq 3$$

Equations (1) are known in literature as *RFM Upward*.

### 1.1 Neural Network Model

Neural Network (NN) approach for geometric calibration purposes of remote sensing images can be considered an innovative and experimental solution. NN are mathematical models which simulate brain dynamics. Computational scheme can be thought as a flow of distributed information which are elaborated within computational node called "neurons" of the NN. Some of them (input) receive data from the external world, some give back information to it (output), some other simply communicate each other (hidden). Neurons are mathematically represented by weights, parameters of the model, which have to be estimated on the basis of the GCP through an iterative learning process. As far as this work is concerned the developed orthorectification procedure is based on an opportunely designed Multi Layer Perceptron (MLP) NN. This type of NN has been chosen for its function approximation and estimation features. It shows its high suitability especially for non linear functions as considered relations are. Basic idea is to substitute the upward projecting model relating image  $(\xi, \eta)$  and ground  $(X, Y, Z)$  coordinate with a well designed and trained MLP NN. NN architecture is the one shown in Figure 4. The most appropriate number of neurons has to be defined time to time according to the number of GCPs and image type. Only an expert user can successfully control it. Indications for the best architecture can be derived from RMSE (Root Mean Square Error) analysis. The NN approach is quite sensible to the initialization of the weights of the neurons.

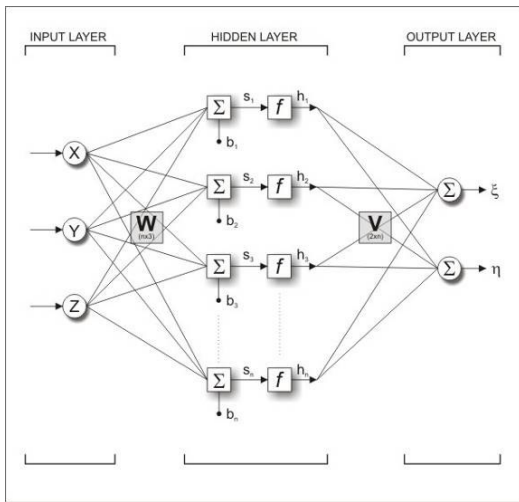


Figure 3 - MLP NN mathematical model with 2 computational layer (*hidden e output*), for the orthorectification problem.

## 3. METHODOLOGY

The methodology for geometric correction on MIVIS images have passed through different tests, entirely performed on MIVIS 1 image. The obtained results were then analyzed from a quantitative and a qualitative point of view to appraise the characteristics of the used methods. The method that guarantees the best performances has been therefore employed for the MIVIS 2 image. This way it allowed the mosaic of MIVIS 1 and 2 images.

### 3.1 GCPs and CPs individualization

GCPs and CPs have been collected on the MIVIS images using both a true colour composite (10-6-1 or 13-7-1) and a single band where a better contrast was necessary. Reference map has been the official orthoimages.

Trying to maintain GCPs and CPs well distributed over the image has been an hard task due to the strength of the original image distortions and to the extended presence of wooded areas. Finally, 72 GCPs and 10 CPs have been collected.

### 3.2 GCPs and CPS elevation extraction

Image coordinates  $(\xi, \eta)$  and planimetric terrain coordinates  $(X, Y)$  of GCPs and CPs derived from official orthoimages, have been completed with the elevation data  $Z$  extracted from the available DEM.

Attainable accuracy in such operation strictly depends on DEM grid dimensions. In this case it is certainly too high considering the mountain test area. In fact, the portion of territory referring to a single cell 50 m x 50 m wide is characterized by a strongly varying height which cannot be properly represented by the univocal value assigned to that cell within the DEM.

To partially solve this problem, the DEM has been resampled to a geometric resolution of 10 m, but tests have demonstrated that this operation does not guarantee a better final result. That's why it has been decided to use for all the performed tests the original DEM.

### 3.3 MIVIS 1 image geometric correction

The followings geometric correction tests have been performed on MIVIS1 image :

- Series 1: RFM method with 20 coefficients varying the number of GCPs: 39, 50, 61, 72;
- Series 2: method based on the NN with 72 GCPs and 10 CPs varying the number of nodes of the hidden layer (from a minimum of 3 to a maximum of 13);
- Series 3: method based on the NN with 10 nodes varying the number of GCPs: 39, 50, 61, 72.

In order to simplify the correction procedure, all the tests have been carried out on three spectral bands out of 102 (bands 10-6-1 were chosen since they produce a good true colour image), using the nearest neighbour resampling method in order minimize image radiometric degradation. Orthoimages geometric resolution has been set equal to 4m as suggested considering the flight height.

### 3.4 Quantitative and qualitative analysis of the results.

The errors achieved, in terms of RMS and residuals on the GCPs and CPs, for every previous tests allow to proceed to a quantitative analysis of the results in order to appraise and

compare, depending on each study images, the characteristics and potentialities of the two geometric correction methods. Particular attention is paid to the following items:

- increasing the number of parameters that define each method (number of polynomial coefficients for the RFM, number of nodes of the hidden layer for the NN) the GCPs errors should decrease (see figure 4);
- increasing the same parameters, the maximum or the minimum difference among the errors on the GCPs and CPs represents an index of the smaller or higher generalization capability of the model (defined as its ability to return correct outputs from different input based on the transformation parameters between image and object coordinates (see figure 4));
- considering a model with good generalization capability, the residuals on the CPs should be higher than those on the GCPs (see figure 4);
- the mean residuals along  $\xi$  and  $\eta$  directions should be null: if not, it's possible to hypothesize the presence of a systematic error in the data and/or in the used correction algorithm;

The results from the quantitative study, based on the previous criterions, must be confirmed by a qualitative analysis, that should verify that:

- the orthorectified image should not present anomalous behaviours as discontinuity or asymptote;
- residuals should be maintained constant on the entire image, also in the areas where the GCPs are not present; this can be done through transparency overlapping, the correspondence of the corrected MIVIS image with the reference map.

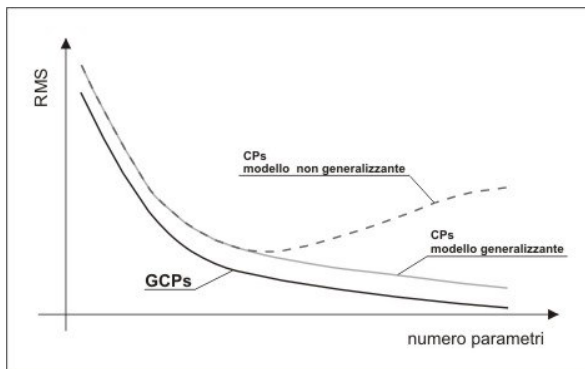


Figure 4 - Relationship between RMS on GCPs and RMS on CPs when evaluating the generalization capacity of the applied model.

At last, a statistic  $\chi^2$  test has been carried out on the GCPs residuals for some of the tests elaborated with RFM and NN methods. This has permitted to verify their adaptation to the expected normal distribution. The test consists in calculating the  $\chi^2$  parameter for the residuals and comparing the obtained value with the theoretical one derived from the defined tables according to the correct degree of freedom and to the chosen level of confidence. If the obtained  $\chi^2$  is smaller than the theoretical one the test is positive, therefore the residuals distribution can be considered to be a normal one. If not it is possible to hypothesize the presence of some systematic phenomena.

### 3.5 Series 1 results analysis

Series 1 tests best results, for the RFM method, have been obtained using a number of coefficients equal to 20. It is therefore possible to think of maintaining such configuration to appraise the characteristics of the model when varying the number N of GCPs as shown in table 3.

R F M 2 0 c o e f f . 1 0 C P s						
GCPs number	RMS $_{\xi}$ (cell n.)		RMS $_{\eta}$ (cell n.)		RMS (cell n.)	
	GCPs	CPs	GCPs	CPs	GCPs	CPs
39	1,85	5,18	3,41	4,14	3,88	6,63
50	1,07	4,19	1,76	2,89	2,06	5,09
61	2,17	4,09	1,91	2,89	2,89	5,01
72	5,56	3,96	2,00	2,50	5,91	4,68
GCPs number	mean Res $_{\xi}$ (cell n.)		mean Res $_{\eta}$ (cell n.)		mean Res (cell n.)	
	GCPs	CPs	GCPs	CPs	GCPs	CPs
39	-0,02	0,49	-0,02	-0,05	3,28	6,16
50	-0,01	-0,69	-0,02	-0,05	1,74	4,18
61	-0,01	1,59	-0,01	0,07	2,44	4,42
72	-0,61	1,19	-0,01	0,15	3,13	4,05

Table 3 – RMS errors and mean residuals for *Serie 2* tests.

Best results are in correspondence of N=61, but it is possible to conclude that RFM method does not seem to be particularly sensitive to the variation of GPC number. However the good numerical results are not confirmed by the qualitative analysis of the corrected images as shown below.

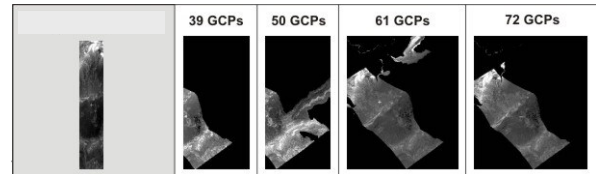


Figure 5 - Geometric correction tests results on MIVIS 1 image by RFM with 20 coefficients when increasing the number of GCPs.

As far as tests performed with the NN approach (table 4) are concerned it is possible to notice that:

1. the RMS error of the GCPs and CPs decreases as the number of nodes increases, both in direction  $\xi$  and  $\eta$  reaching a stable value in correspondence of 7 nodes;
2. the RMS of the CPs remain similar as the ones on the GCPs;
3. the worst behaviour is not obvious along  $\xi$  for the RFM method;
4. the mean residuals along  $\xi$  and  $\eta$  direction are null for the GCPs, while for the CPs, even though not reaching elevated values, they are slightly away from zero.



Neural Nets 72 GCPs and 10 CPs						
Nodes number	RMS <sub>ξ</sub> (cell n.)		RMS <sub>η</sub> (cell n.)		RMS (cell n.)	
	GCPs	CPs	GCPs	CPs	GCPs	CPs
3	12,32	12,85	16,61	17,01	20,68	21,32
4	5,40	7,86	11,57	8,09	12,77	11,28
5	4,24	4,14	11,57	7,64	12,33	8,69
6	4,00	5,43	8,14	7,26	9,07	9,07
7	1,43	1,89	4,33	3,01	4,56	3,55
8	1,58	2,14	6,17	4,04	6,37	4,57
9	1,14	2,09	3,82	3,57	3,99	4,14
10	0,77	1,61	2,44	3,67	2,56	4,00
11	0,70	1,32	3,80	4,06	3,86	4,27
12	0,66	1,65	2,94	3,83	3,01	4,17
13	0,42	1,34	2,26	3,03	2,29	3,32
Nodes number	mean Res <sub>ξ</sub> (n. celle)		mean Res <sub>η</sub> (n. celle)		mean Res (n. celle)	
	GCPs	CPs	GCPs	CPs	GCPs	CPs
3	0,00	-3,64	0,00	-1,75	16,99	17,64
4	0,00	-1,79	0,00	0,27	10,97	10,08
5	0,00	-1,07	0,00	-0,93	10,16	7,53
6	0,00	-2,51	-0,15	0,56	7,70	8,42
7	0,00	-1,39	0,00	-0,30	3,68	3,19
8	0,00	-0,83	0,00	-0,34	5,25	3,91
9	0,00	-1,18	0,00	-0,23	3,41	3,76
10	0,00	-1,07	0,00	-0,51	2,17	3,21
11	0,00	-0,49	0,00	-0,93	3,06	3,69
12	0,00	-0,07	0,00	-0,58	2,36	3,79
13	0,00	-0,14	0,00	-0,97	1,82	2,96

Table 4 – RMS and mean residuals obtained from Series 2 test.

The RMS behaviour for the GCPs and CPs, seems to suggest a good generalization capability while the number of nodes increases.

The general qualitative analysis confirm that the corrected images do not introduce particular anomalies (see Figure 6).

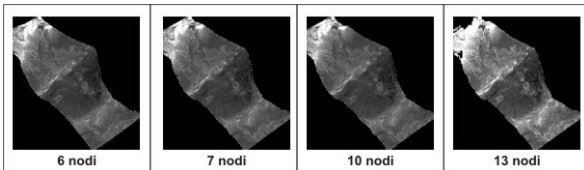


Figure 6 – Images obtained from NN test on series 2 while increasing the nodes.

Only in a few cases we have noticed some small discontinuities at the upper limits of the image, however these are entirely negligible in comparison to those found in the RFM method.

On the other hand the overlap of the map furnishes satisfactory results as well (in each test the accuracy is constant throughout the entire image, also along the uneven zones where the GCP are not present) and confirms the previous errors, above 7 nodes the improvements are limited and located only to some points (see Figure 7).

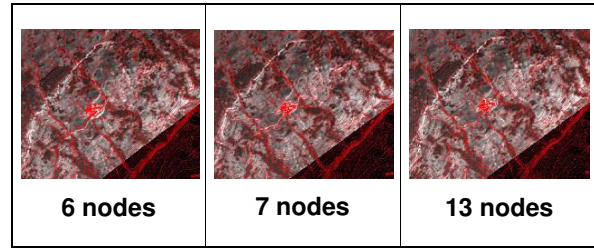


Figure 6 – Images obtained from NN test with nodes increases and cartographic map overlap results.

### 3.7 Series 3 analysis results

As for the RFM method now it is possible to evaluate the sensibility of the NN method while varying the number of GCPs for a constant number of nodes (10).

The results in correspondence of the four different configurations of points (the same used for Series 1) are shown in table 5. From their analysis it is not possible to deduce a direct dependence of the level of attainable accuracy with the number of GCPs, all the RMS maintain very similar each other. This is also confirmed by the qualitative analyses. The best configuration is N=61, as for the RFM..

Neural Nets 10 nodes and 10CPs						
GCPs number	RMS <sub>ξ</sub> (cell n.)		RMS <sub>η</sub> (cell n.)		RMS (cell n.)	
	GCPs	CPs	GCPs	CPs	GCPs	CPs
39	0,16	5,76	2,49	5,37	2,49	7,87
50	0,58	3,44	4,46	4,30	4,49	5,50
61	0,75	1,76	3,02	2,38	3,12	2,96
72	0,77	1,61	2,44	3,67	2,56	4,00
GCPs number	mean Res <sub>ξ</sub> (cell n.)		mean Res <sub>η</sub> (cell n.)		mean Res (cell n.)	
	GCPs	CPs	GCPs	CPs	GCPs	CPs
39	0,00	1,75	0,00	-0,36	2,04	6,81
50	0,00	-0,88	0,00	-0,47	3,83	4,99
61	0,00	-0,97	0,00	-0,91	2,51	2,32
72	0,00	-1,07	0,00	-0,51	2,17	3,21

Table 5 – RMS and means of residuals obtained from the Series 3 tests.

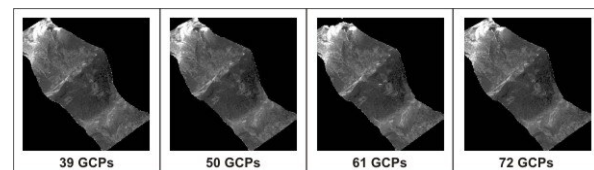


Figure 7 – Images obtained with the NN correction approach on Series 3 while increasing the GCPs.

### 3.8 Normality Test on the residuals

The  $\chi^2$  test on the residuals has been carried out on the following tests:

- RFM with 20 coefficients and 72 GCPs;
- NN with 10 nodes and 72 GCPs.

The test has been positive for the residuals obtained with the NN approach. Residuals along  $\xi$  direction obtained with the RFM method do not pass the test; a systematic effect can be hypothesized in this case.

### 4. CONCLUSIONS

The obtained results from the performed tests allow to conclude that:

- RFM method introduces instability problems when using third order polynomials, underlined quantitatively by the elevated variability values of RMS and qualitatively by the presence of strong anomalies in the corrected images;
- such anomalies are not present if the NN approach is adopted;
- the RFM method shows the worst behaviour along  $\xi$  (also confirmed by the results of the residuals normality test), not underlined by the other two methods; it could be due to a unknown systematic errors induced on the data by the MIVIS whiskbroom scanning system or by the correction method itself;
- the method based on the NN shows good generalization capabilities when observing the decreasing number of errors on the GCPs and CPs as the number of parameters grow, not observed for the other two methods;
- the level of attainable accuracy from the two methods can be judged as good. Also considering that the qualitative analyses have often revealed that it is greater than the RMS numerical values suggested.

### 5. MIVIS 2 IMAGE GEOMETRIC CORRECTION AND MOSAICKING

MIVIS 2 image has been corrected using NN method and 72 GCPs. Therefore MIVIS 1 and MIVIS 2 NN orthorectified images have been linked in a mosaic. The final result is shown in the final figure showing good coherence.



### References

- Bello, M. G. , 1992, Enhanced training algorithms, and integrated training/architecture selection for multilayer perceptron networks, *IEEE Trans. on Neural Networks*, 3,864-875.
- Borgogno Mondino E., Giardino M., Perotti L. - *Neural Network : a method for the application of hyperspectral images analysis to the Cassas landslide hazard assessments (Susa Valley, NW-Italy)* 1° EGU, Nice 2004.
- Breuer M., Albertz J., Geometric Correction of airborne whiskbroom scanner imagery using hybrid auxiliary data, in *IAPRS - International Archives of Photogrammetry and Remote Sensing*, vol. XXXIII, 2000.
- Demouth H., Beale M., *Neural Network Toolbox User's Guide*, vol. 4, Matlab, 2003.
- Dowman, I., Tao, V., 2002, An update on the use of rational functions for photogrammetric restitution, *ISPRS, Vol. 7, N°3*, September 2002, pp. 26-29
- Giardino M., Gomasca Mario A., Piero Boccoardo, Enrico Borgogno Mondino, Luigi Perotti *Airborne Sensor Mivis Images For Landslide Phenomena Analysis In Mountain Areas* 5th ISEMG, Thessaloniki, Greece 2004.
- Howard Demuth, Mark Beale, *MATLAB Neural Network Toolbox User's Guide*, The Mathworks, Version 4, pp.5-8,5-30.
- Tao, C., Hu, Y., 2001, A comprehensive study of the Rational Function Model for Photogrammetric processing, *Photogrammetric engineering & Remote Sensing*, December 2001, pp.1347-1357.